

Adsorption-Controlled Growth of Perovskite Oxides for Optimized Opto-Electric Properties

Viviana Glick^a, Dylan Sotir^{b,c}, Darrell Schlom^{b,d,e}

^aDepartment of Chemistry, Haverford College, Haverford, 19041, Pennsylvania, USA ^bDepartment of Materials Science and Engineering, Cornell University, Ithaca, 14853, New York, USA ^cPlatform for the Accelerated Realization, Analysis, and Discovery of Interface Materials (PARADIM), Cornell University, Ithaca, New York 14853, USA ^dKavli Institute at Cornell for Nanoscale Science, Ithaca, 14853, New York, USA ^eLeibniz-Institut für Kristallzüchtung, Max-Born-Str. 2, 12489 Berlin, Germany

Abstract

Barium strontium titanate (BST) is an attractive material to be used as a tunable pseudo substrate for strain engineering perovskite thin-films. BST's adjustable lattice parameters (3.9-4.0 Å) enable high-quality film growth on cost-effective substrates. Using adsorption-controlled growth with molecular beam epitaxy (MBE), we can achieve stoichiometrically pure films¹ by leveraging a laser heater for precise pressure-temperature conditions. Ellingham-esque diagrams can be used to guide phase-pure growth. Experiments show SrTiO₃ nucleates as islands, transitioning to smooth films at 14 nm, with growth influenced by thickness and temperature, and optimal growth temperature at 1475 °C. These findings contribute to the development of highly ordered perovskite films for advanced technological applications.

1. Introduction

Perovskite oxides are a class of materials possessing many interesting and highly tunable opto-electric properties, making them attractive for a broad range of technological applications, such as quantum computing and solar cells.^{2,3} High quality crystal structures are necessary in order to utilize these properties. Perovskite oxide films are thus grown on top of crystalline substrates to encourage the growth of highly ordered films. By choosing a substrate with a specific lattice mismatch relative to the film, we can strategically strain the film to optimize its strain-dependent properties. The lattice parameters of the substrate must be similar to those of the desired film in order to induce film strain, but with too much of a mismatch, the film will grow relaxed on top of the substrate. Fine-tuning film strain, or a lack thereof, requires substrates with specific lattice parameters.

Barium strontium titanate (Ba_xSr_{1-x}TiO₃, or BST) is a cubic perovskite oxide that can be grown as a pseudo substrate: a thick relaxed film grown for use as a substrate for another film to be grown on top of. BST has a tunable lattice constant dependent on the Ba:Sr ratio, or x . This allows for the growth of BST with a lattice constant ranging from 3.9-4.0 Å, a region within which many perovskites of interest are grown. BST is thus useful for fine-tuning the strain of many highly studied perovskites for desired properties. The use of BST as a pseudo substrate

would allow for the growth of high quality films without necessitating the purchase of expensive high quality substrates.

In order to both make effective pseudo substrates and optimize the opto-electric properties of the films grown on top of them, films of high stoichiometric purity are needed. As a basis for growing BST pseudo substrates, SrTiO₃ (STO) was grown, which is equivalent to BST with $x = 0$. Perfectly calibrating each elemental source in Molecular-Beam Epitaxy (MBE) is nearly impossible, causing imperfections in films grown. To address this, self-limiting growth can be achieved with adsorption-control: one elemental source in the MBE is much more volatile than the rest, so when the volatile source is oversupplied, it adsorbs onto the growing film surface, incorporating only where needed stoichiometrically, and excess volatile material desorbs back off, to yield theoretically perfect film stoichiometry. The volatility of each source is dependent on the pressure and temperature conditions within the growth chamber. Ellingham-esque diagrams can be calculated and used to guide growths (**Figure 1**).

Traditional MBE systems can only reach temperatures up to ~1000°C. To remain within the ideal pressure-temperature growth window for STO, these temperatures necessitate pressures too low to

accurately calibrate during growth, on the bottom right of the highlighted region in **Figure 1**.

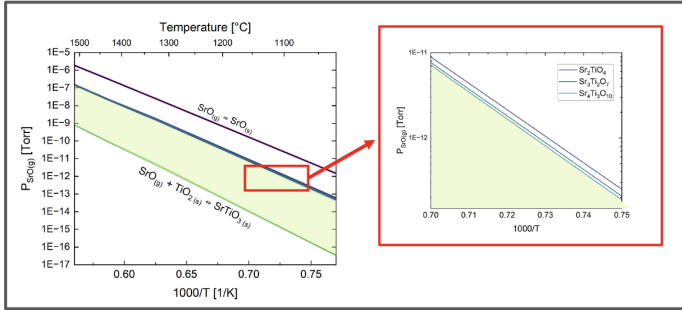


Figure 1: Ellingham-esque Diagram for STO

The calculated phase-pure growth window for STO (113) is highlighted in green. Outside this region we expect to see impurities. The magnified region on the right shows the Ruddelston-Popper phases, STO (2 1 4), (3 2 7), and (4 3 10), expected at the edge of this highlighted window.

More volatile organic precursor sources can also be used,⁴ but they clog the system, yielding imperfect films. However, using a laser heater, temperatures up to $\sim 2100^\circ\text{C}$ can be achieved, allowing for growth at higher pressures which can be accurately calibrated, resulting in high quality growth.

2. Methods

2.1: Growth Window Ellingham Diagrams

Pressure-temperature growth windows for phase-pure material were calculated from the Gibbs free energy of each material in the chemical reaction of interest at a range of temperatures.^{5,6} The reaction quotient, Q , was found from $Q = e^{\Delta G/RT}$. The pressure of the system was then found by taking $1/Q$, and translating from bar to torr. These calculations were done for SrTiO_3 , BaZrO_3 , CaZrO_3 , and SrZrO_3 , as well as for $\text{Pb}(\text{Ti}_{1-x}\text{Zr}_x)\text{O}_3$ for x values of 0 and 1.

Since pressure cannot be calibrated directly during growth but flux at the film surface can, partial pressure was translated to SrO overflux at the substrate surface, using the equation $\Gamma = P \sqrt{N_A / [2\pi M k_B T]}$ where Γ is SrO overflux, P is SrO partial pressure, N_A is Avagadro's number, M is SrO molar mass, k_B is the Boltzmann constant, and T is the temperature (K).

2.2: Adsorption-controlled STO growth with MBE

All films were grown on LaAlO_3 (LAO) (100) using molecular-beam epitaxy (MBE) with laser-heated Sr, Ti, and O_3 sources. Sr was supplied in excess in a 5:1 Sr:Ti ratio. Growth rate was determined for each run with timed calibrations and thicknesses determined

with X-Ray Reflectivity (XRR). STO thin-films were first grown at 33 nm thick at temperatures ranging from $1350\text{-}1550^\circ\text{C}$. An 8 nm sample was grown at 1475°C to examine STO nucleation and surface morphology. A thickness series was performed at 1475°C , with 6-25 nm thicknesses and a temperature series was performed at 10 nm thick at temperatures between $1425\text{-}1525^\circ\text{C}$. Reflection High-Energy Electron Diffraction (RHEED) tracked surface quality during film growth to inform MBE source calibrations. Film purity was measured with X-Ray Diffraction (XRD) and surface topography was investigated via Atomic Force Microscopy (AFM). Lattice strain was measured with Reciprocal Space Mapping (RSM).

3. Results and Discussion

The 33 nm thick sample at 1475°C was a high-quality film with a high-quality relaxed film smooth surface (515 pm RMS roughness) and desired step formations (**Figure 2a**). In contrast, the 8 nm sample with the same growth conditions shows STO nucleation as disconnected islands (**Figure 2b**).

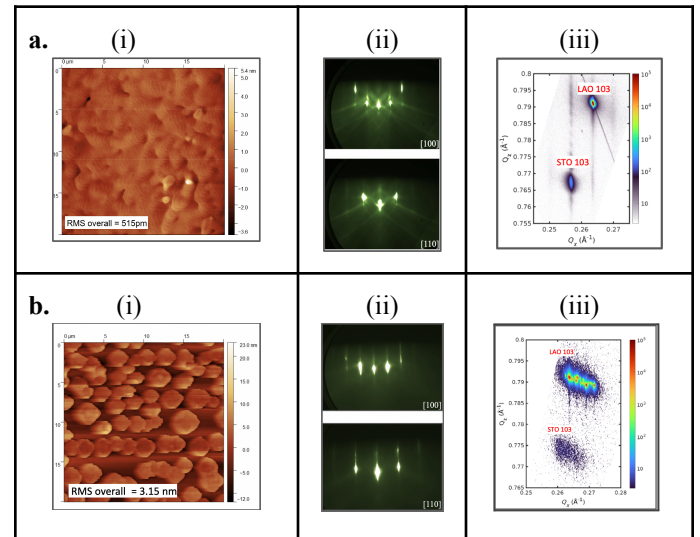


Figure 2: Effect of Thickness on Nucleation of STO

AFM, RHEED, and RSM data (from left to right) are shown for two samples of STO grown on LAO substrates at 1475°C . For sample (a) (33 nm thick), AFM (a (i)) shows a smooth stepped surface, ideal for stepwise growth. The 5 closely spaced and clear intensities at the 100 azimuth and 3 broadly spaced intensities at the 110 azimuth of the RHEED (a (ii)) indicate cubic symmetry and the sharp features and Kikuchi lines indicate a smooth surface and highly ordered film surface. The misalignment of the LAO substrate and STO film in the RSM (a (iii)) indicates a relaxed film. For sample (b) (8 nm thick), the AFM (b (i)) shows STO nucleating as islands, with a high surface roughness over 46% of the film thickness, indicating irregular crystal growth and poor film quality. The RHEED (b (ii)) pattern shows cubic symmetry and the intensities are relatively clear, but the lack of Kikuchi lines indicates lower surface crystal ordering than in sample (a). The RSM (b (iii)) for sample (b) shows twinning in the LAO substrate, indicated by the many RSM peaks, interfering with crystal quality of the film grown on top. Although the film and substrate peaks are vaguely aligned, no strain can be determined due to the poor definition of both.

A thickness series (selected AFM in **Figure 3**) investigated the transition between island nucleation

and smooth film growth. At 6 nm, STO nucleated as islands, which began merging at 8 nm. At 14 nm, steps began to form and RMS roughness dropped by over 50%, after which it gradually declined with smoother surfaces and clearer stepping at 17 and 20 nm. The globular nature of the steps seen here resembles the islands, indicating that STO nucleates as islands, which merge together and form steps with increased thickness, starting around 14 nm.

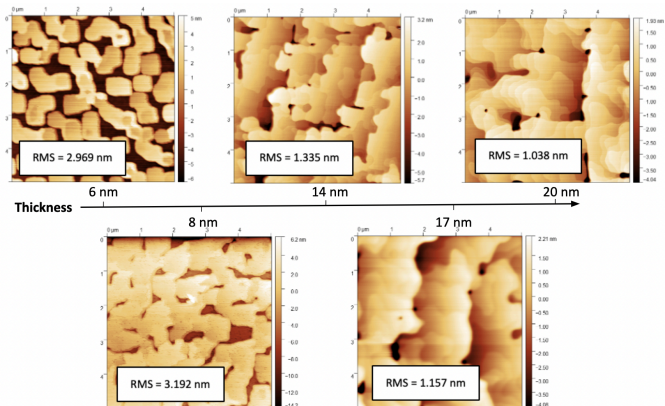


Figure 3: Thickness Series
5 micron AFM images are shown for samples grown at 1475°C at varying thicknesses to observe the effect of film thickness on STO nucleation.

To explore the effect of temperature on STO film growth, a temperature series was taken (**Figure 4**). Temperature results were less conclusive, but STO did nucleate as islands at 1425 °C, merging at 1450 °C and 1475 °C to yield a smoother surface. Unexpected results were observed at 1500 °C. We conjecture that the round shapes are STO islands as seen before, the square shapes are TiO₂ or very Ti-rich STO clusters, and the cross shapes remain a mystery. Further analysis is necessary to determine the film makeup.

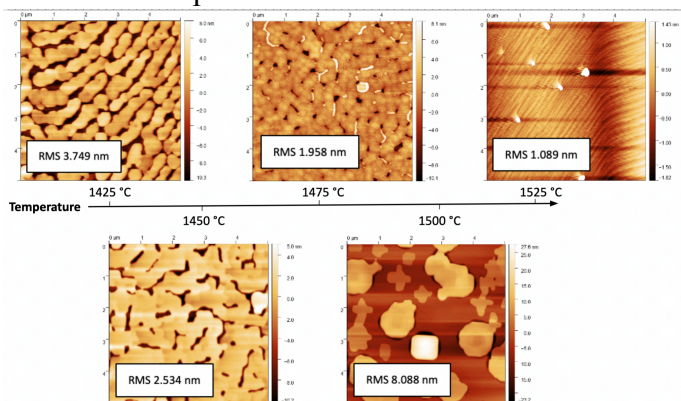


Figure 4: Temperature Series
5 micron AFM images are shown for 10 nm thick samples grown at varying temperatures to observe the effect of film temperature on STO nucleation.

At 1525 °C, the surface texture nearly disappears,

possibly due to substrate and film interdiffusion. Although phase-pure 33 nm SrTiO₃ films were previously at 1525 °C, the temperature series consisted of only 10 nm samples, so it is possible that this behavior was occurring in the thicker samples as well before final thickness was reached.

4. Conclusion

STO nucleation was investigated at varied temperatures and thicknesses. STO appears to nucleate from islands that merge around 1475 °C and steps begin to form when film thickness reaches ~14 nm. Future STO work could include growing at different growth rates. A combined understanding of STO and BaTiO₃ (BTO) can be implemented to grow BST pseudosubstrates. Ellingham-esque diagrams were successfully used to predict the phase-pure growth window for SrTiO₃ and to inform experiments. Similar calculations were performed for zirconates of similar structure and lead zirconium titanate, and the same methods can be applied to other systems, which could then be explored experimentally.

5. Acknowledgements

I would like to thank my mentor Dylan Sotir and PI Dr. Darrell G. Schlom for the opportunity to be a part of this project and for their guidance throughout it, as well as the Platform for the Accelerated Realization, Analysis, and Discovery of Interface Materials (PARADIM) grant from the National Science Foundation (NSF) for funding this research.

6. Works Cited

- (1) Jalan, B.; Moetafak, P.; Stemmer, S. Molecular Beam Epitaxy of SrTiO₃ with a Growth Window. *Appl. Phys. Lett.* 2009, 95 (3), 032906. <https://doi.org/10.1063/1.3184767>.
- (2) Hensling, F. V. E.; Braun, W.; Kim, D. Y.; Majer, L. N.; Smink, S.; Faeth, B. D.; Mannhart, J. State of the Art, Trends, and Opportunities for Oxide Epitaxy. *APL Mater.* 2024, 12 (4), 040902. <https://doi.org/10.1063/5.0196883>.
- (3) Mesquita, W. D.; de Jesus, S. R.; Oliveira, M. C.; Ribeiro, R. A. P.; de Cássia Santos, M. R.; Junior, M. G.; Longo, E.; do Carmo Gurgel, M. F. Barium Strontium Titanate-Based Perovskite Materials from DFT Perspective: Assessing the Structural, Electronic, Vibrational, Dielectric and Energetic Properties. *Theor. Chem. Acc.* 2021, 140 (3), 27. <https://doi.org/10.1007/s00214-021-02723-2>.
- (4) Tejedor, P.; Benedicto, M.; Vázquez, L.; Galiana, B. Nucleation Kinetics of SrTiO₃ 3D Islands and Nanorings on Si Substrates. *Nanoscale* 2014, 6 (21), 13188–13195. <https://doi.org/10.1039/C4NR04416A>.
- (5) B-Br2, Ca-CeTe, Si-SrWO₄, Ta-Th2N2O, and WS2-e. In *Thermochemical Data of Pure Substances*; John Wiley & Sons, Ltd, 1995; pp 104–208, 416–523, 1480–1586, 1587–1655, and 1815–1885. <https://doi.org/10.1002/9783527619825.ch12e>.
- (6) Thomas C. Allison. NIST-JANAF Thermochemical Tables - SRD 13, 2013. <https://doi.org/10.18434/T42S31>.